

Pressure-induced structural transition of $Y_2Zr_2O_7$

HPSTAR
267-2016



Hui Li^a, Qiang Tao^a, Nana Li^b, Ruilian Tang^b, Yongsheng Zhao^a, Hongyu Zhu^a,
Pinwen Zhu^{a,*}, Xin Wang^{a,*}

^a State Key Laboratory of Superhard Materials, Jilin University, Changchun 130012, China

^b Center for High Pressure Science and Technology Advanced Research, Shanghai 201203, China

ARTICLE INFO

Article history:

Received 30 October 2015

Received in revised form

17 November 2015

Accepted 19 November 2015

Available online 2 December 2015

Keywords:

$Y_2Zr_2O_7$

Defect fluorite

High-pressure

Structural phase transition

ABSTRACT

The structural changes of $Y_2Zr_2O_7$ under high pressure have been investigated by using angle-dispersive synchrotron X-ray powder diffraction up to 34 GPa at room temperature. A new pressure-induced phase transition from cubic ($Fm-3m$) structure to orthorhombic ($Pnma$) structure at 27.3 GPa is observed, and the phase transition is irreversible. The high-pressure orthorhombic ($Pnma$) phase has longer average cation–anion bonding distance than cubic ($Fm-3m$) structure which was proved by the increase of coordination number.

© 2015 Elsevier B.V. All rights reserved.

1. Introduction

The pyrochlore-structured materials with the general formula $A_2B_2O_7$, where A is rare earth including the lanthanides, Y, sometimes Sc and B is either a transition metal or a *p*-block metal ion, have received intense interest for many researchers over decades [1]. Now there are hundreds of various synthetic compounds with pyrochlore structure. Diverse chemical composition makes pyrochlore showing a diversity of material properties. For example, in electricity, $Cd_2Re_2O_7$ exhibited superconductivity at 1.1 K [2], $Pr_2Ir_2O_7$ showed unconventional anomalous Hall effect [3], $Cd_2Os_2O_7$ underwent a metal-insulator transition (MIT) near 226 K [4]. Besides, pyrochlore-structured materials being highly geometrically frustrated exhibit very rich exotic magnetic phenomena [5], which included spin glass behavior in $Y_2Mo_2O_7$ [6], spin ice in $Ho_2Ti_2O_7$, $Dy_2Ti_2O_7$, $Dy_2Ti_2O_7$, and $Ho_2Sn_2O_7$ [1,7], and long-range order (LRO) with persistent low-temperature spin dynamics in $Gd_2Sn_2O_7$ and $Er_2Ti_2O_7$ [7–9].

Among these oxides, the rare-earth zirconates with the formula $A_2Zr_2O_7$ especially attract our attention because there are a variety of potential applications for these materials. For example, $Gd_2Zr_2O_7$ is highly radiation resistant making it an important nuclear

material [10–12]; $La_2Zr_2O_7$ is a prominent photoelectrochemical catalyst [13], and it is also used as thermal barrier coating because of the high melting points [14]; $Ce_2Zr_2O_7$ is considered for possible application in magnetohydrodynamic (MHD) power generation [15]. These applications require materials capable to withstand harsh environments, so the studies on the stability of these materials under extreme condition (i.e., irradiation, high temperature, and high pressure) are particularly important.

The rare-earth zirconates $A_2Zr_2O_7$ present as one of two closely related isometric structures at ambient conditions [16], which is closely related to the ionic radius ratio of $r(A^{3+})/r(Zr^{4+})$. The pyrochlore structure (space group: $Fd-3m$) stability at atmospheric pressure is limited to the range of $1.46 \leq r(A^{3+})/r(Zr^{4+}) \leq 1.78$, in which the A and Zr cations occupy 16d and 16c site, respectively and the O has two crystallographically distinct oxygen sites (48f, 8b). The defect fluorite structure (space group: $Fm-3m$) can form for $r(A^{3+})/r(Zr^{4+}) < 1.46$, in which the cations and anions are randomly distributed on the positions of 4a and 8c, respectively, with one eighth of the anion positions vacant as compared with ideal fluorite structure (AX_2) [17]. The phase transition from the $Fd-3m$ pyrochlore structure to the $Fm-3m$ defect fluorite structure is an order–disorder transition, which involves the disordering of the anions among the 48f, 8b sites and the vacant 8a site, as well as the disordering of the cations at 16c and 16d sites. Temperature can induce order–disorder phase transition in rare-earth zirconate pyrochlores, which has been studied by spectroscopy and

* Corresponding author.

** Corresponding author.

E-mail addresses: zhupw@jlu.edu.cn (P. Zhu), xin_wang@jlu.edu.cn (X. Wang).

transmission electron microscopy [18–20].

Pressure plays an important role in the structural stability of materials. Recent experimental and theoretical studies have reported a phase transformation and amorphization of zirconates at around 15–30 GPa [21–27]. For example, the ordered pyrochlore $\text{Gd}_2\text{Zr}_2\text{O}_7$ transformed to a distorted defect-fluorite structure above 15 GPa [24], similar to the case under irradiation [28]; at pressures above 18 GPa, a pressure-induced phase transition occurred for $\text{Sm}_2\text{Zr}_2\text{O}_7$ that studied by angle-dispersive X-ray diffraction (ADXRD) and Raman scattering methods [22]; the corresponding transition pressures were 21 and 22 GPa for $\text{La}_2\text{Zr}_2\text{O}_7$, $\text{Nd}_2\text{Zr}_2\text{O}_7$, respectively [26,27]. So far, the above discussions are the study of pyrochlore oxides at high pressures, while the defect-fluorite oxides have the very similar structural stability and high pressure behavior as the pyrochlore structure oxides. It has reported a defect-fluorite to a cotunnitelike phase transformation at pressures of ~22 and ~30 GPa for $\text{Er}_2\text{Zr}_2\text{O}_7$ and $\text{Ho}_2\text{Zr}_2\text{O}_7$, respectively. Enhanced compressibility was found for the high pressure phase as a result of increasing cation coordination number and peculiar cation–anion bond length increasing was uncovered [23]. However, no more other reports of this kind of high pressure transition in experiments, the high pressure transformation mechanism is still unclear, further more study to understand peculiar cation–anion bond length increasing under high pressure is necessary. Recently first-principles calculations [17] predicted that defect-fluorite (F-type) $\text{Y}_2\text{Zr}_2\text{O}_7$ could transform to the defect-cotunnite (C-type) structure at ~18 GPa which were accompanied by enhanced compressibility, increased average cation–anion bonding distance and decreased band gap. However, till now, there have been no reports about experimental studies of pressure-induced phase transition for the defect-fluorite $\text{Y}_2\text{Zr}_2\text{O}_7$. It is significant to study the high pressure behavior of $\text{Y}_2\text{Zr}_2\text{O}_7$ to uncover transformation mechanism and understand peculiar cation–anion bond length increasing.

In this study, the high pressure structural response of $\text{Y}_2\text{Zr}_2\text{O}_7$ is studied by in situ X-ray diffraction (XRD) measurements. A new high pressure C-type phase is found at 27.3 GPa. Moreover, exotic cation–anion bond length increasing is found and attributed to increasing cation coordination number. These results are consistent with other previously studied oxides and the theoretical study of $\text{Y}_2\text{Zr}_2\text{O}_7$.

2. Experimental methods

The $\text{Y}_2\text{Zr}_2\text{O}_7$ compound was synthesized by standard solid state reaction method. Stoichiometric quantities of Y_2O_3 (99.99%) and ZrO_2 (AR) were mixed thoroughly together in an agate mortar. The obtained powder was pressed into small pellets and calcined at 1773 K in air for 12 h.

At ambient condition, the phase purity was detected by powder XRD measurements using Rigaku Rotaflex X-ray diffractometer with $\text{Cu-K}\alpha$ radiation at room temperature. In situ ADXRD experimental runs were carried out at BLX17C of National Synchrotron Light Source at Brookhaven using the angle-dispersive XRD mode ($\lambda = 0.4073 \text{ \AA}$). One piece of the as-prepared samples was loaded into a gasketed diamond-anvil cell (DAC) with a 16:3:1 methanol/ethanol/water mixture as pressure-transmitting medium. The pressure in our experiments was measured by ruby method [29]. The experimental parameters including the distance between sample and detector were calibrated using the CeO_2 standard material. Two-dimensional XRD images were analyzed using the FIT2D software, yielding one-dimensional intensity versus diffraction angle 2θ patterns. Rietveld analyses were performed with the software GSAS [30].

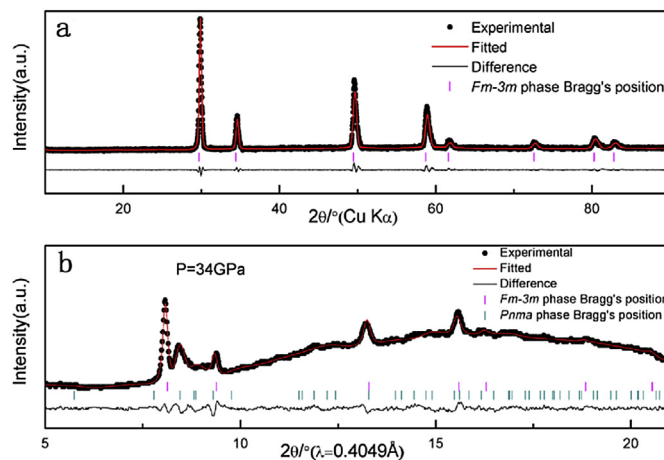


Fig. 1. (a) Rietveld refinement of $\text{Y}_2\text{Zr}_2\text{O}_7$ at ambient pressure in cubic ($Fm\bar{3}m$) phase. (b) Rietveld refinement of $\text{Y}_2\text{Zr}_2\text{O}_7$ at 34 GPa in orthorhombic ($Pnma$) phase.

3. Results and discussion

3.1. X-ray diffraction patterns at ambient pressure

The crystal structure data were refined by Rietveld analysis of the X-ray powder diffraction data with GSAS software. The observed and calculated XRD patterns along with the difference plot are shown in Fig. 1a and the merit of the refinement is $R_p = 7.7\%$, $R_{wp} = 8.4\%$ at ambient pressure. The diffraction peaks match well with the cubic structure (S.G. $Fm\bar{3}m$, No.225) and the obtained cell parameters are: $a = 5.2165(6) \text{ \AA}$. The refined atomic position coordinates are given in Table 1. The schematic diagram of the defect-fluorite $\text{Y}_2\text{Zr}_2\text{O}_7$ structure is presented in Fig. 2a.

3.2. High pressure X-ray diffraction

Selected XRD patterns of $\text{Y}_2\text{Zr}_2\text{O}_7$ up to 34 GPa are shown in Fig. 3. From ambient pressure up to 25.7 GPa, the patterns exhibit a typical defect-fluorite structure. It can also be seen that all diffraction peaks markedly shift to larger diffraction angles as pressure increases. At 27.3 GPa, a new high-pressure (HP) phase appears, and this HP phase coexists with the defect-fluorite structure up to 34 GPa. It suggests a substantial kinetic barrier for this transformation. Also, the phase transition is irreversible as the diffraction peaks of the HP structure remains after complete release of pressure.

The structural response of other closely related compounds at pressure was studied by in situ X-ray diffraction measurements. For example, CaF_2 (ideal fluorite structure) transformed to a

Table 1

The refined atomic coordinates of the ambient pressure cubic phase and the high pressure orthorhombic phase of $\text{Y}_2\text{Zr}_2\text{O}_7$ at 27.3 GPa.

Compounds	$\text{Y}_2\text{Zr}_2\text{O}_7$ (at ambient pressure)	$\text{Y}_2\text{Zr}_2\text{O}_7$ (27.3 GPa)
Crystal system	Cubic	Orthorhombic
Space group	$Fm\bar{3}m(225)$	$Pnma(62)$
a/Å	5.2165(6)	5.862(8)
b/Å	5.2165(6)	3.041(3)
c/Å	5.2165(6)	6.312(5)
Atoms	Wyckoff (x y z)	Wyckoff (x y z)
Y(Zr)	4a (0 0 0)	4c (0.2600 0.2500 0.3873)
O(1)	8c (0.25 0.25 0.25)	4c (0.0284 0.2500 0.6785)
O(2)		4c (0.1444 0.2500 0.0721)

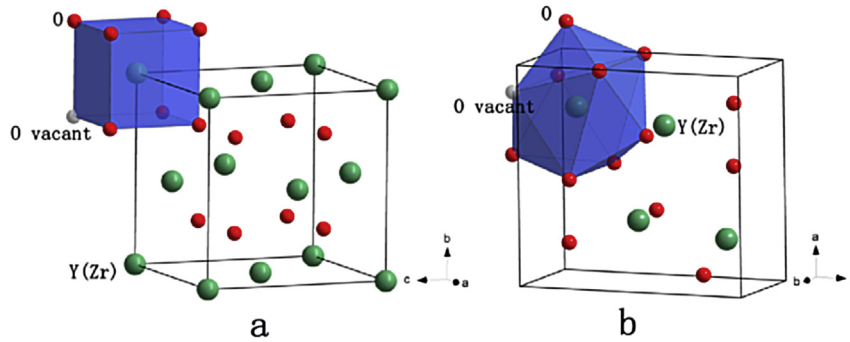


Fig. 2. (a) Structural schematic diagrams of the defect-fluorite $Y_2Zr_2O_7$. (b) Structural schematic diagrams of the defect-cotunnite $Y_2Zr_2O_7$ high-pressure phase.

denser structure type, orthorhombic $PbCl_2$ type, at about 9.5 GPa [31], which was similar with BaF_2 , UO_2 and ThO_2 [32,33]. $Er_2Zr_2O_7$ and $Ho_2Zr_2O_7$ with defect-fluorite structure under ambient conditions could transform to defect-cotunnite structure at high pressure [23]. Besides, Xiao et al. showed the defect-cotunnite structure was more stable at high pressure than defect-fluorite structure in $Y_2Zr_2O_7$ [17]. The theoretical value of pressure-induced phase transition from defect-fluorite to defect-cotunnite structure was 18 GPa, while the starting transition pressure to the high-pressure phase was ~ 27.3 GPa from this experiment. And the observed XRD patterns of the high-pressure phase in Fig. 3 were quite similar to the patterns of the high-pressure phase of $Er_2Zr_2O_7$ and $Ho_2Zr_2O_7$. Therefore, we can speculate that the HP phase of $Y_2Zr_2O_7$ is defect-cotunnite structure. Rietveld refinements of two phases were carried out by using GSAS software. The results of $Y_2Zr_2O_7$ at 34 GPa are shown in Fig. 1b, which is in good agreement with the predication. The refinement is converged with the agreement factors: $R_p = 0.78\%$, $R_{wp} = 1.17\%$. In defect-cotunnite structure, both cations and anions are randomly distributed on $4c$ positions and one eighth of the anions are missing. The atomic structure of the cotunnite-type unit cell is shown in Fig. 2b and the determined structural parameters are listed in Table 1. For both structures with one eighth of the anion positions vacant, the cation coordination number (CN) is 7 in defect-fluorite structure and 8 in defect-cotunnite structure,

which can be clearly seen from Fig. 2. The cations in both phases are in a close-packed arrangement: cubic in defect-fluorite structure, hexagonal in defect-cotunnite structure, and it is occupied by a very narrow range of structural distortions, as shown by their lattice parameters a , b , and c . The axial ratios a/b and c/b are 1.928 and 2.075 at 27.3 GPa, which are higher than the ratios expected for ideal hexagonal close-packing [34]. Applying high pressure makes the undistorted cation packing in defect-fluorite structure transform to the distorted cation packing in defect-cotunnite structure.

Because of potential applications for electrolyte materials, the ionic conductivity of $Y_2Zr_2O_7$ has been extensively studied, which showed that doping and temperature can change its conductivity [35,36]. Norby also found that the structural order–disorder transition had a direct impact on the conductivity in $Y_2(Ti_{1-x}Zr_x)_2O_7$ system [37]. To be sure, the structural changes will bring about changes in the conductivity under pressure. Therefore, the electrical measurement of $Y_2Zr_2O_7$ at high pressures will be our future work.

The pressure dependences of the unit volume of $Y_2Zr_2O_7$ up to 34 GPa are shown in Fig. 4, in which the volume of the unit cell decreases by approximately 9.0% during the F- \rightarrow C-type phase transition at 27.3 GPa, however the theoretical value is 14.3%. The actual volume change is less, and the observation is usually attributed to the repulsive effects of atoms being forced together into a more highly coordinated environment. This is a smaller

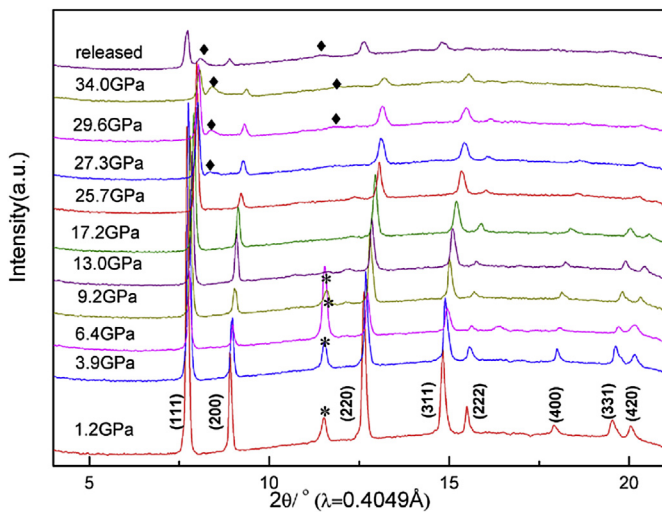


Fig. 3. X-ray diffraction patterns of $Y_2Zr_2O_7$ as a function of increasing pressure. The top pattern was taken from the quenched samples after the release of pressure. The black rhombus represents the diffraction peaks from the high-pressure phase. The asterisks mark the diffraction peaks from the gasket.

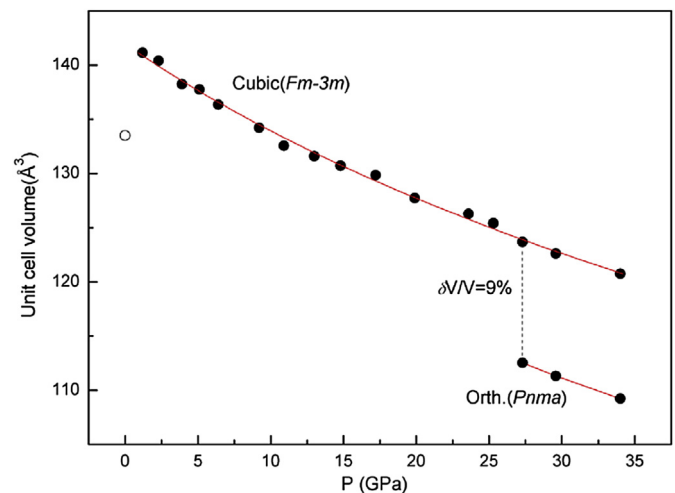


Fig. 4. Pressure dependence of the unit cell volume derived from the observed XRD patterns by the Rietveld refinement method (Closed circles, compression). Open circles, decompression).

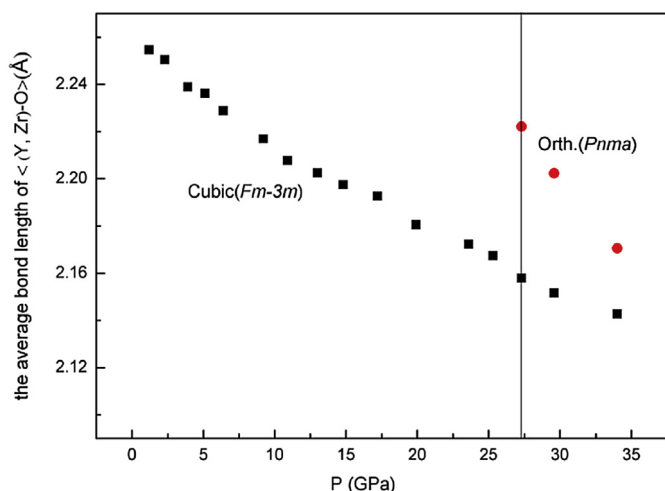


Fig. 5. Variation of the average bond length of $\langle Y, Zr-O \rangle$ of the defect-fluorite $Y_2Zr_2O_7$ structure and the cotunnite-type as a function of pressure.

volume change that is observed for many other high pressure phase transitions involving a coordination change [34]. The equation of state was fitted by a second-order Birch–Murnaghan equation of state [38]:

$$P = \frac{3.0}{2} B_0 \left[\left(\frac{V_0}{V} \right)^{\frac{2}{3}} - \left(\frac{V_0}{V} \right)^{\frac{5}{3}} \right] \times \left(1 + \frac{3.0}{4} (B'_0 - 4) \times \left[\left(\frac{V_0}{V} \right)^{\frac{2}{3}} - 1 \right] \right) \quad (1)$$

Where B_0 is the bulk modulus and B'_0 is its pressure derivative at the equilibrium volume V_0 . The bulk modulus of B_0 is 153(3) GPa for the cubic ($Fm-3m$) phase with fixed $B'_0 = 4$. The value of the bulk moduli is significantly less than other $A_2Zr_2O_7$ with defect-fluorite structure, for example, the bulk modulus of $Ho_2Zr_2O_7$ and $Er_2Zr_2O_7$ are 238(9) and 279(6) GPa, respectively [23].

The pressure dependences of $\langle Y, Zr-O \rangle$ bond distance are shown in Fig. 5, indicating that the bond distance of the F-type $Y_2Zr_2O_7$ decreases smoothly with increasing pressure, which is uniquely determined by the unit cell parameter. However, the average cation–anion bonding distance increases from 2.15 to 2.22 Å for F-type to C-type transformation in $Y_2Zr_2O_7$ at 27.3 GPa, and it indicates that the ionic bonds in C-type is weaker than F-type. The intrinsic reason of longer ionic bonds in C-type is attributed to the increase of CN, the cation CN is 7 in defect-fluorite structure and 8 in defect-cotunnite structures. Per atom of Y (Zr) in C-type cannot provide enough electrons as F-type due to higher CN, so ionic bonds are weaker and longer in C-type. The variation tendency of $\langle Y, Zr-O \rangle$ bond distance is almost consistent with the theoretical study [17].

4. Conclusion

The F-type $Y_2Zr_2O_7$ was prepared by standard solid state reaction method. The high-pressure behaviors of this compound have been investigated by angle-dispersive synchrotron X-ray powder diffraction at room temperature and a pressure-induced phase transition from F-type structure to C-type structure at 27.3 GPa was observed. The bulk modulus (B_0) is determined to be 153(3) GPa for the F-type structure by fitting the pressure–volume data using the Birch–Murnaghan equation of state. The $\langle Y, Zr-O \rangle$ bond distance increases from 2.15 to 2.22 Å during the phase transition at

27.3 GPa, which is due to the increase in the coordination number. This work studies the high pressure behavior of $Y_2Zr_2O_7$ and it is significant to further understand fluorite oxides at high pressures.

Acknowledgment

This work was financially supported by the National Natural Science Foundation of China under Grant No. 51172091, the Program for New Century Excellent Talents in University, China (NCET-12-0240), Jilin Province Science and Technology Development Program, China (20130101023JC). We acknowledge Dr. Chen Zhi-qiang for technical support with the high pressure experiments at the BLX17C of the NSLS synchrotron.

References

- [1] J.S. Gardner, M.J. Gingras, J.E. Greedan, *Rev. Mod. Phys.* 82 (2010) 53–107.
- [2] M. Hanawa, Y. Muraoka, T. Tayama, T. Sakakibara, J. Yamaura, Z. Hiroi, *Phys. Rev. Lett.* 87 (2001) 187001.
- [3] Y. Machida, S. Nakatsui, Y. Maeno, T. Tayama, T. Sakakibara, S. Onoda, *Phys. Rev. Lett.* 98 (2007) 057203.
- [4] D. Mandrus, J.R. Thompson, R. Gaal, L. Forro, J.C. Bryan, B.C. Chakoumakos, L.M. Woods, B.C. Sales, R.S. Fishman, V. Keppens, *Phys. Rev. B* 63 (2001) 195104.
- [5] J.E. Greedan, *J. Alloys Compd.* 408–412 (2006) 444–455.
- [6] M.J.P. Gingras, C.V. Stager, N.P. Raju, B.D. Gaulin, J.E. Greedan, *Phys. Rev. Lett.* 78 (1997) 947.
- [7] S.T. Bramwell, M.J. Gingras, *Science* 294 (2001) 1495–1501.
- [8] Y. Chapuis, P. Dalmas de Réotier, C. Marin, A. Yaouanc, A. Forget, A. Amato, C. Baines, *Phys. B* 404 (2009) 686–688.
- [9] J. Lago, T. Lancaster, S.J. Blundell, S.T. Bramwell, F.L. Pratt, M. Shirai, C. Baines, *J. Phys. Condens. Matter* 17 (2005) 979–988.
- [10] K.E. Sickafus, L. Minervini, R.W. Grimes, J.A. Valdez, M. Ishimaru, F. Li, K.J. McClellan, T. Hartmann, *Science* 289 (2000) 748–751.
- [11] R.C. Ewing, W.J. Weber, J. Lian, *J. Appl. Phys.* 95 (2004) 5949–5971.
- [12] A. Chartier, G. Catillon, J.P. Crocombette, *Phys. Rev. Lett.* 102 (2009) 155503.
- [13] T. Omata, S. Otsuka-Yao-Matsuo, *J. Electrochem. Soc.* 148 (2001) E475–E482.
- [14] H. Zhou, D. Yi, Z. Yu, L. Xiao, *J. Alloys Compd.* 438 (2007) 217–221.
- [15] R.A. Chapman, D.B. Meadowcroft, A.J. Walkden, *J. Phys. D Appl. Phys.* 3 (1970) 307–319.
- [16] M.A. Subramanian, G. Aravamudan, G.V. Subba Rao, *Prog. Solid State Chem.* 15 (1983) 55–143.
- [17] H.Y. Xiao, F. Gao, W.J. Weber, *Phys. Rev. B* 80 (2009) 212102.
- [18] Y.H. Lee, H.S. Sheub, J.P. Denga, H.-C.I. Kao, *J. Alloys Compd.* 487 (2009) 595–598.
- [19] D. Michel, M. Perez, Y. Jorba, R. Collongues, *Mater. Res. Bull.* 9 (1974) 1457–1468.
- [20] E.I. Zoz, A.M. Gavrish, N.V. Gul'ko, *Inorg. Mater.* 14 (1978) 109–111.
- [21] F.X. Zhang, J.W. Wang, J. Lian, M.K. Lang, U. Becker, R.C. Ewing, *Phys. Rev. Lett.* 100 (2008) 045503.
- [22] F.X. Zhang, J. Lian, U. Becker, L.M. Wang, J.Z. Hu, S. Saxena, R.C. Ewing, *Chem. Phys. Lett.* 441 (2007) 216–220.
- [23] F.X. Zhang, M. Lang, U. Becker, R.C. Ewing, J. Lian, *Appl. Phys. Lett.* 92 (2008) 011909.
- [24] F.X. Zhang, J. Lian, U. Becker, R.C. Ewing, J.Z. Hu, S.K. Saxena, *Phys. Rev. B* 76 (2007) 214104.
- [25] N.R.S. Kumar, N.V.C. Shekar, P.C. Sahu, *Solid State Commun.* 147 (2008) 357–359.
- [26] F.X. Zhang, M. Lang, Zhenxian Liu, R.C. Ewing, *Phys. Rev. Lett.* 105 (2010) 015503.
- [27] H.Y. Xiao, F.X. Zhang, Fei Gao, M. Lang, Rodney C. Ewing, W.J. Weber, *Phys. Chem. Chem. Phys.* 12 (2010) 12472–12477.
- [28] S.X. Wang, B.D. Begg, L.M. Wang, R.C. Ewing, W.J. Weber, K.V. Govindan Kutty, *J. Mater. Res.* 14 (1999) 4470–4473.
- [29] H.K. Mao, J. Xu, P.M. Bell, *J. Geophys. Res.* 91 (1986) 4673–4676.
- [30] A.C. Larson, R.B. Von Dreele, *General Structure Analysis System, LANSCE, MS-H805, Los Alamos, New Mexico, 1994.*
- [31] L. Gerward, J.S. Olsen, S. Steenstrup, M. Malinowski, S. Åsbrink, A. Waskowska, *J. Appl. Cryst.* 25 (1992) 578–581.
- [32] J.M. Leger, J. Haines, A. Atouf, O. Schulte, *Phys. Rev. B* 52 (1995) 13247–13256.
- [33] M. Idiri, T. Le Bihan, S. Heathman, J. Rebizant, *Phys. Rev. B* 70 (2004) 014113.
- [34] E. Morris, T. Groy, K. Leinenweber, *J. Phys. Chem. Solids* 62 (2001) 1117–1122.
- [35] M. Kumar, M. Anbu Kulandainathan, I. Arul Raj, R. Chandrasekaran, R. Pattabiraman, *Mater. Chem. Phys.* 92 (2005) 295–302.
- [36] M. Kumar, I. Arul Raj, R. Pattabiraman, *Mater. Chem. Phys.* 108 (2008) 102–108.
- [37] T. Norby, *J. Mater. Chem.* 11 (2001) 11–18.
- [38] F. Birch, *J. Geophys. Res.* 83 (1978) 1257–1268.